BMC Microbiology

RESEARCH

Open Access

NagPIBAF upregulation and *ompO* downregulation compromise oxidative stress tolerance of *Stenotrophomonas maltophilia*

Tsuey-Ching Yang[1], Shao-Chi Wu[1], Ting-Yu Yeh[1], Hsu-Feng Lu[2], Yi-Tsung Lin[3,4] and Li-Hua Li[5,6*]

Abstract

Background Outer membrane protein OmpA is composed of two domains, an N-terminal β-barrel structure embedded in the outer membrane and a C-terminal globular domain noncovalently associated with the peptidoglycan layer in periplasm. *Stenotrophomonas maltophilia* KJ is a clinical isolate. In our recent study, we disclosed that KJΔOmpA$_{299-356,}$ an OmpA C-terminal deletion mutant, compromised menadione tolerance. Furthermore, the involvement of σ^E, σ^N, and *ompO* in the Δ*ompA*$_{299-356}$-mediated phenotype was proposed. In that study, we hypothesized that there was an unidentified σ^N-regulated candidate responsible for Δ*ompA*$_{299-356}$-mediated menadione tolerance decrease, and the candidate was disclosed in this study.

Methods and results Transcriptome analysis of wild-type KJ and KJΔOmpA$_{299-356}$ revealed that a five-gene cluster, *smlt4023-smlt4019* (annotated as *nagPIBAF*), was upregulated in KJΔOmpA$_{299-356}$. Reverse transcription-PCR (RT-PCR) confirmed the presence of the *nagPIBAF* operon. The expression of the *nagPIBAF* operon was negatively regulated by NagI and σ^N, and triggered by *N*-acetylglucosamine. In-frame deletion mutant construction and menadione tolerance assay demonstrated that *nagP*, *nagB*, and *nagA* upregulation in KJΔOmpA$_{299-356}$ connected with Δ*ompA*$_{299-356}$-mediated menadione tolerance decrease. The intracellular reactive oxygen species (ROS) level assay further verified that in the presence of external oxidative stress such as menadione treatment, *nagPIBAF* operon upregulation and *ompO* inactivation synergistically increased intracellular ROS levels, which exceeded the capacity of bacterial oxidative stress alleviation systems and resulted in a decrease of menadione tolerance.

Conclusions Loss of interaction between OmpA C-terminus and peptidoglycan causes envelope stress and activates σ^E regulon. *ompO* and *rpoN* are downregulated in response to σ^E activation. *rpoN* downregulation further derepresses *nagPIBAF* operon, which can favor the metabolism route of glycolysis, TCA cycle, and electron transport chain. *nagPIBAF* upregulation and OmpO downregulation synergistically increase intracellular ROS levels and result in menadione tolerance decrease.

Clinical trial number Not applicable.

Keywords *Stenotrophomonas maltophilia*, Oxidative stress, *N*-acetylglucosamine utilization

*Correspondence:
Li-Hua Li
lilh@vghtpe.gov.tw

Full list of author information is available at the end of the article

Background

Bacteria derive the energy required for growth through a considerable number of diverse reactions. ATP generated by the metabolic route of glycolysis-citric acid cycle-electron transport chain is a major energy source for aerobic pathogens. However, ROS are inevitable byproducts of aerobic respiration, imposing oxidative stress on pathogens. Aerobic metabolism-generated ROS include superoxide radical ($O_2^{-\bullet}$), hydrogen peroxide (H_2O_2), and hydroxyl radical (HO•). Furthermore, redox enzymes can accidentally transfer electrons to oxygen instead of to their proper substrates, thereby increasing the formation of superoxides and hydrogen peroxide [1]. In addition to endogenous ROS, pathogens encounter high levels of superoxide radicals generated by phagocytes in mammalian hosts [2]. ROS can cause the nonspecific oxidation of biomolecules, making them toxic to bacteria. To survive, bacteria have acquired several alleviation systems to deal with oxidative stress. Strategies by which pathogens minimize ROS-mediated injuries include scavenging and repair systems. Detoxifying enzymatic systems (superoxide dismutase, catalase, hydroperoxide reductase, and peroxidase) and export systems (efflux pumps and outer member porins) are the main ROS-scavenging systems. Once biomolecules are oxidized, repair systems can reverse the damaged biomolecules to their active state [3]. Examples include excision and recombination repair systems for DNA damage, and thioredoxin, glutaredoxin, and reductase systems for protein damage [4]. For energy availability, bacteria have developed several mechanisms which allow the preferred utilization of the most efficiently metabolizable carbohydrates in their ecological niche. *N*-acetylglucosamine (GlcNAc) is a glucose derivative that is an important carbon and nitrogen source and a structural component of bacterial peptidoglycan (PG) [5, 6]. In bacteria, GlcNAc can be endogenously produced by PG recycling, or exogenously imported from the extracellular environment (Fig. 1). The bacterial PG monomer is composed of a sugar backbone, alternating β-(1,4)-linked GlcNAc and *N*-acetylmuramic acid

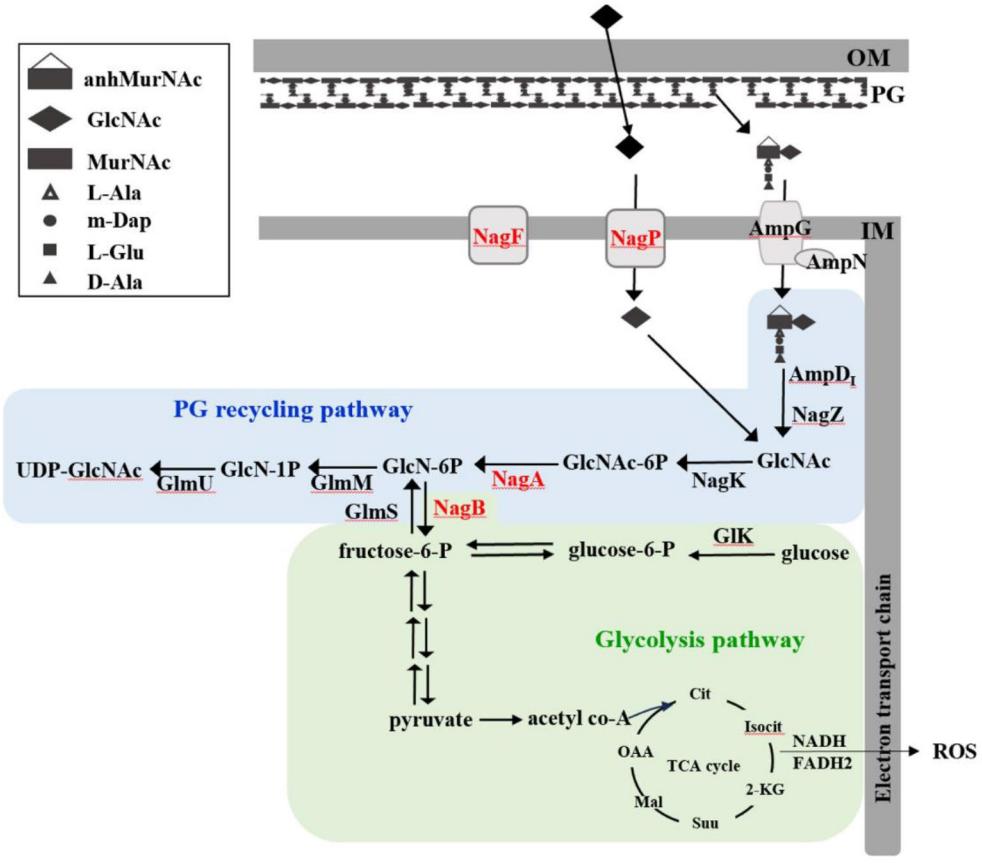

Fig. 1 Interconnection of PG recycling and glycolysis pathways in *S. maltophilia*. During PG turnover, GlcNAc-β-anhMurNAc-peptides are generated by the cleavage of lytic transglycosylases and transported into the cytoplasm via the inner membrane AmpNG permease system. GlcNAc-β-anhMurNAc-peptides are hydrolyzed into GlcNAc by NagZ. GlcNAc is phosphorylated and deacetylated by NagK and NagA, respectively, generating GlcN-6P. GlcN-6P, the key molecule at the intersection of the PG recycling and glycolysis pathways, can be driven into the PG recycling pathway by the GlmM-GlmU system or directed into the glycolysis pathway under the action of NagB. The pathways marked in blue and green represent PG recycling and glycolysis, respectively. Proteins encoded by the *nagPIBAF* operon are marked in red

(MurNAc), and five amino acids attached to MurNAc [6]. During PG turnover, pre-existing PG is cleaved by lytic transglycosylases to generate GlcNAc-β-anhMurNAc-peptides in the periplasm. GlcNAc-β-anhMurNAc-peptides are transported to the cytosol by the inner membrane AmpG permease system. GlcNAc is then generated from GlcNAc-β-anhMurNAc-peptides via *N*-acetyl-β-glucosaminidase (NagZ) hydrolysis [7]. Additionally, GlcNAc can be imported from the environment via a specific inner membrane phosphotransferase system (PTS) such as NagE in *Escherichia coli* [8], ATP-binding cassette (ABC) transporters such as NgcEFG in *Streptomyces olivaceoviridis* [9], or major facilitator superfamily (MFS) transporters such as NagP in *Xanthomonas campestris* [10]. GlcNAc transported through the PTS is coupled with phosphorylation and that transported by the MFS is phosphorylated in the cytoplasm by glucokinase family proteins to generate GlcNAc-6P. GlcNAc-6P is deacetylated by *N*-acetylglucosamine-6-phosphate deacetylase (NagA) to glucosamine-6-phosphate (GlcN-6P). GlcN-6P is used in the catabolic pathways that drive GlcN-6P into the glycolysis pathway via the glucosamine 6-phosphate deaminase (NagB) or is shunted into the anabolic pathways that create UDP-GlcNAc via the NagA-GlmM-GlmU system [10] (Fig. 1). When GlcN-6P is favored by NagB, the generated fructose-6-P enters the glycolysis, which can lead to the increase of ROS level (Fig. 1).

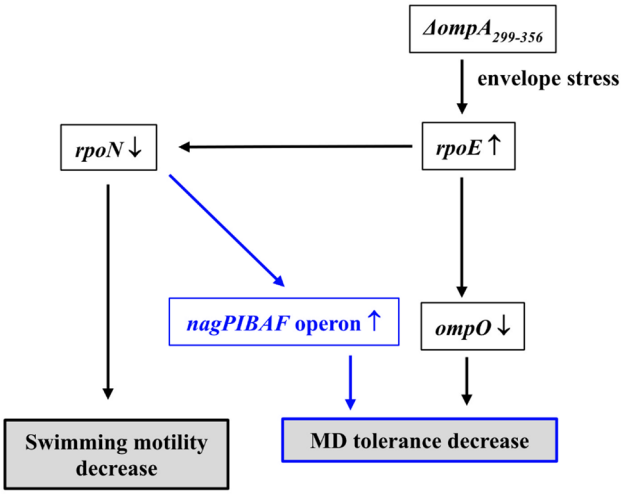

Fig. 2 The proposed mechanism model responsible for the Δ$ompA_{299-356}$-mediated decrease of MD tolerance and swimming motility in *Stenotrophomonas maltophilia* KJ. The words, arrows, and symbols marked in black indicate the known mechanism reported in our previous study (Liao et al., 2021; Ku et al., 2023). The words, arrows, and symbols marked in blue indicate the novel findings in this study. The OmpA protein of KJΔ$OmpA_{299-356}$ is devoid of 299–356 amino acids, which is the key domain for the interaction of OmpA and PG. Owing to the loss of OmpA-PG contact, KJΔ$OmpA_{299-356}$ experiences an envelope stress, activating σ^E. Sigma E activation downregulates the expression of *ompO* and *rpoN*. Downregulated σ^N leads to the swimming motility defect and upregulates *nagPIBAF* operon. OmpO downregulation and *nagPIBAF* upregulation collectively lead to the Δ$ompA_{299-356}$-mediated decrease of MD tolerance

OmpA, a β-barrel porin, is the most abundant outer membrane protein (OMP) in most Gram-negative bacteria. The N-terminus of OmpA forms a β-barrel structure, which is embedded in the outer membrane functioning as a channel for the influx or efflux of molecules. The C-terminal globular domain of OmpA is suspended in the periplasm and non-covalently associated with the PG layer [11–12]. OmpA is involved in many functions, such as adhesion, serum resistance, biofilm formation, a receptor for pilus, and immune target, which appear to be more relevant to the N-terminal β-barrel domain of OmpA [13–14]. Loss of the C-terminal domain of OmpA is linked to a compromise in signal transduction and integrity of the outer membrane and PG [15].

Stenotrophomonas maltophilia is a gram-negative, non-fermenting bacterium that is ubiquitously distributed in nature, including in soil, animals, plant roots, and aqueous environments. Additionally, *S. maltophilia* is an opportunistic pathogen prone to infections in immunocompromised patients. Like most gram-negative bacteria, OmpA was the most abundant OMP in *S. maltophilia* KJ. Distinct from the classical outer membrane porins (such as OmpF), the C-terminal domain of OmpA is unique. KJΔ$OmpA_{299-356,}$ an *ompA* in-frame deletion mutant of *S. maltophilia* KJ, was constructed in a previous study [16]. The OmpA encoded by KJΔ$OmpA_{299-356}$ keeps an intact N-terminal-barrel embedded in the outer membranes but loses contact with PG. KJΔ$OmpA_{299-356}$ displays pleiotropic defects, including compromise in conjugation ability, swimming motility, β-lactam resistance, and oxidative stress tolerance. The underlying mechanism responsible for the Δ$ompA_{299-356}$-mediated pleiotropic defects was revealed [16–18]. Menadione (MD), a superoxide generator, is used as an agent to induce oxidative stress. Based on our previous studies, we propose a mechanism to explain the Δ$ompA_{299-356}$-mediated decrease of MD tolerance [18] Fig. 2). Owing to the loss of the OmpA-PG interaction, KJΔ$OmpA_{299-356}$ experiences envelope stress, resulting in σ^E activation, which downregulates *ompO* and *rpoN* expression. Sigma N downregulation compromises swimming motility [16]. Furthermore, *rpoN* and *ompO* downregulation contribute to Δ$ompA_{299-356}$-mediated decrease of MD tolerance [18]Fig. 2). Because *ompO* is not a member of σ^N regulon [18], we speculated that there should be an unidentified candidate, which is regulated by σ^N, linked to the Δ$ompA_{299-356}$-mediated decrease of MD tolerance. In this study, we further elucidated that the *nagPIBAF* operon, a member of σ^N regulon, is involved in the Δ$ompA_{299-356}$-mediated decrease of MD toleranceFig. 2).

Methods

Bacterial strains and plasmids

Bacterial strains and plasmids used were listed in Supplemental Table 1. The primers used in this study were listed in Supplemental Table 2.

Reverse-transcription PCR and operon verification

DNA-free RNA was isolated from KJΔOmpA$_{299-356}$ cells and subjected to reverse transcription using the NagF-C primer. The cDNA was used as the template for PCR using the primer sets NagPQ95-F/R, NagIQ92-F/R, NagBQ103-F/R, NagAQ103-F/R, and NagFQ106-F/R (Supplemental Table 2). PCR products were separated by 2% agarose gel electrophoresis and visible by ethidium bromide staining.

Construction of in-frame deletion mutants

In-frame deletion mutants were constructed using the strategy of double cross-over homologous recombination as described previously [19]. Two DNA fragments upstream and downstream of the intended deleted gene were amplified from the chromosome of *S. maltophilia* KJ via PCR. The primer sets used were listed in Supplemental Table 2. Two PCR amplicons were subsequently cloned into pEX18Tc to generate pEX18Tc-derived recombinant plasmids (Supplemental Table 1) and then these plasmids were introduced into *S. maltophilia* KJ via conjugation. Transconjugants were selected on LB plates supplemented with norfloxacin (2.5 μg/mL) and tetracycline (30 μg/mL). Then, the deletion mutant was selected by spreading the transconjugants onto 10% sucrose-containing LB plate. The correctness of deletion mutant was checked by PCR and sequencing [19].

Menadione tolerance assay

The logarithmic-phase bacterial cells of 2×10^5 CFU/μL were serially 10-fold diluted. Five microliter bacterial aliquot was spotted onto LB agar with and without menadione. After a 24-h incubation at 37°C, the cell viabilities were recorded.

Construction of the promoter-*xylE* transcriptional fusion constructs, pNagP$_{xylE}$ pNagI$_{xylE}$, and pOmpO$_{xylE}$

The putative promoter region upstream of *nagP* gene was predicted via website https://www.fruitfly.org/seq_tools/promoter.html and the predicted promoter region located 55–104 bp upstream of *nagP* gene. The 390-bp DNA fragment upstream of *nagP* was PCR amplified using NagPN-F/R primers (Supplemental Table 2) and cloned into pXylE [20] to generate pNagP$_{xylE}$ (Supplemental Table 1). Similar strategy for the construction of pNagI$_{xylE}$ and pOmpO$_{xylE}$. The 444-bp and 356-bp DNA fragments upstream of *nagI* and *ompO* were PCR amplified using NagPN-F/R and OmpON-F/R primers (Supplemental Table 2) and cloned into pXylE to yield pNagI$_{xylE}$ and pOmpO$_{xylE}$ (Supplemental Table 1), respectively.

Catechol-2,3-dioxygenase (C23O) activity determination

The activity of catechol-2,3-dioxygenase (C23O) encoded by *xylE* gene serves as a reporter for monitoring the promoter activity. C23O activity was determined spectrophotometrically at 375 nm using catechol as a substrate as described previously [21]. One unit of enzyme activity (U) was defined as the amount of enzyme that converts 1 nmol of catechol per minute. Specific activity (U/OD$_{450}$) of the enzyme was defined in terms of units per OD$_{450nm}$ unit of cells. All experiments were performed in triplicates.

Intracellular ROS level determination (DCFH-DA assay)

Bacterial cells were inoculated into fresh LB broth at an initial OD$_{450nm}$ of 0.15. After 4-h culture, 2',7'-Dichlorodihydrofluorescein Diacetate (DCFH-DA) [22] was added to a final concentration 0.01 μM and then incubated for further 1 h. The fluorescence intensity was measured at 488 nm excitation and 520 nm emission. Bacterial mass was determined by recording the optical density at 450 nm (OD$_{450nm}$). Intracellular ROS level was expressed as fluorescence intensity/OD$_{450nm}$.

Results

The *nagPIBAF* operon upregulation contributes to the Δ*ompA*$_{299-356}$-mediated decrease of oxidative stress tolerance

Oxidative stress can be attributed to the decrease of ROS alleviation ability and the increase of ROS production. In our recent study, we reported that downregulation of an OMP OmpO is involved in Δ*ompA*$_{299-356}$-mediated decrease of MD tolerance [16, Fig. 2], which highly is linked to the decrease of ROS alleviation ability. Herein, we further considered whether the increase of ROS production is also involved in *DompA*$_{299-356}$-mediated decrease of MD tolerance. To identify the putative candidate(s), we surveyed the transcriptome results of wild-type KJ and KJΔOmpA$_{299-356}$ [16]. We defined the significant difference as an absolute fold change in TPM equal to or greater than three. Given that ROS are inevitable byproducts of the metabolic route of glycolysis-citric acid cycle-electron transport chain in an aerobic pathogen [23], the genes involved in this metabolic route were surveyed. We noticed that a five-gene cluster, Smlt4023-Smlt4019 (Fig. 3), was upregulated in KJΔOmpA$_{299-356}$ (Table 1). Based on the findings of this study, we designated Smlt4023-4019 as *nagP-nagI-nagB-nagA-nagF* (Fig. 3). The reliability of the transcriptome results was confirmed by qRT-PCR, and results demonstrated that *nagA* transcript in KJΔOmpA$_{299-356}$ had a 4.4 ± 0.5-fold

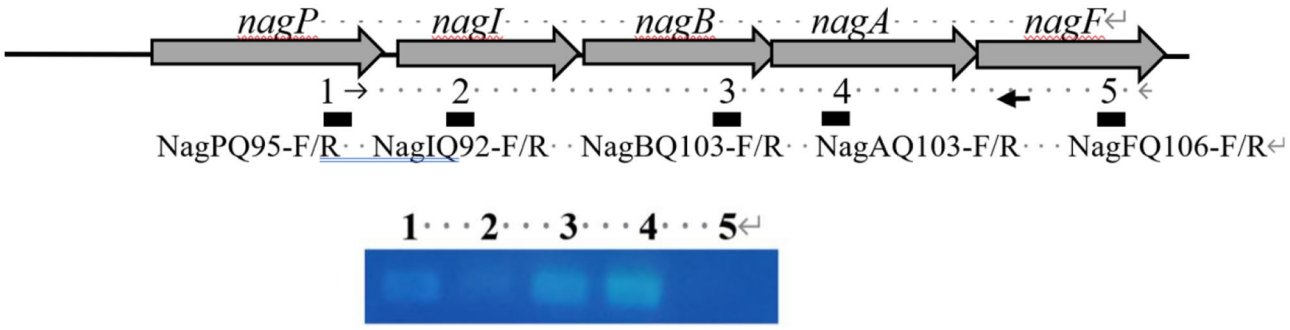

Fig. 3 *NagPIBAF* is an operon. The cDNAs of KJΔOmpA$_{299-356}$ were obtained by RT-PCR using the primer NagF-C and used as the template for the following PCR. The location of primer NagF-C for RT-PCR is indicated by the black arrow. Solid bars (labeled as 1 to 5) indicate the locations of PCR amplicon using the primer pairs labeled below. The PCR amplicons were separated by agarose gel electrophoresis and then stained with ethidium bromide. Lane 1, PCR amplicon generated by NagPQ95-F/R; Lane 2, PCR amplicon generated by NagIQ92-F/R; Lane 3, PCR amplicon generated by NagBQ103-F/R; Lane 4, PCR amplicon generated by NagAQ103-F/R; Lane 5, PCR amplicon generated by NagFQ106-F/R (as a negative control)

Table 1 Transcriptome analysis of *nagPIBAF* operon in wild-type KJ and *ompA* mutant, KJΔOmpA$_{299-356}$

Locus	Protein	TPM		Fold change
		KJ	KJΔOmpA$_{299-356}$	
Smlt4019	NagF	20.87	90.53	+4.34
Smlt4020	NagA	31.80	147.72	+4.65
Smlt4021	NagB	37.41	166.99	+4.46
Smlt4022	NagI	30.50	131.24	+4.30
Smlt4023	NagP	51.51	183.50	+3.56

[a]TPM, Transcripts Per Kilobase Million

[b]Negative fold changes represent genes that were significantly downregulated in KJΔOmpA$_{299-356}$, whereas positive fold changes represent upregulation in KJΔOmpA$_{299-356}$

increase compared to that in wild-type KJ (Supplemental Fig. 1), verifying the reliability of transcriptome analysis. We investigated whether *nagP-nagI-nagB-nagA-nagF* overexpression contributes to Δ*ompA*$_{299-356}$-mediated decrease of oxidative stress tolerance. To address this, five genes were deleted from KJΔOmpA$_{299-356}$ to generate KJΔNagPIBAFΔOmpA$_{299-356}$. A *ompA* complementary strain KJL2::OmpAΔOmpA$_{299-356}$ [16] was included for comparison. Compared to KJΔOmpA$_{299-356}$, the MD tolerance of KJΔNagPIBAFΔOmpA$_{299-356}$ was restored to the wild-type level (Fig. 4), indicating that the five-gene cluster upregulation contributes to Δ*ompA*$_{299-356}$-mediated decrease of MD tolerance. Furthermore, the *nagA* transcript in KJL2-OmpAΔOmpA$_{299-356}$, an *ompA* complementation strain of KJΔOmpA$_{299-356}$ [17], was reverted to the wild-type level (Supplemental Fig. 1), ensuring the link between OmpA mutant and *nag* operon upregulation.

Given their genomic organization and simultaneous upregulation in KJΔOmpA$_{299-356}$, *nagP*, *nagI*, *nagB*, *nagA*, and n*agF* were highly organized into an operon. To test this possibility, DNA-free RNA was purified from KJΔOmpA$_{299-356}$ cells and subjected to RT-PCR. These results confirm the presence of *the nagPIBAF* operon (*nag* operon for short hereafter) (Fig. 3).

The proteins encoded by the *nag* operon appear to be a GlcNAc utilization system. The protein encoded by *nagP* was annotated as an MFS inner membrane transporter and displayed 82% identity with NagP of *X. campestris*. The 355-aa NagI contains two domains: an N-terminal helix-turn-helix DNA-binding domain of the LacI family (1–70 residues) and a C-terminal ligand-binding domain (70–340 residues). Protein encoded by *nagB* is annotated as glucosamine-6-phosphate deaminase (NagB), which catalyzes the conversion of GlcN-6-P to fructose-6-phosphate. *NagA* encodes *N*-acetylglucosamine-6-phosphate deacetylase (NagA), which catalyzes the deacetylation of *N*-acetylglucosamine-6-phosphate (GlcNAc-6P) to glucosamine-6-phosphate (GlcN-6-P). NagF is predicted to be an inner membrane protein with nine transmembrane domains, including a heparan-α-glucosaminide-*N*-acetyltransferase domain. To test the contribution of *nag* operon to GlcNAc utilization, the growth of wild-type KJ and KJΔNagPIBAF was spectrometrically monitored in minimal medium XOLN supplemented with GlcNAc as the sole carbon source (XOLN-GlcNAc medium). As can be seen in Supplemental Fig. 2, wild-type KJ grew well in XOLN-GlcNAc medium, but KJΔNagPIBAF lost viabilities, indicating that *nag* operon contributes to GlcNAc utilization in *S. maltophilia*.

NagPIBAF operon is repressed by NagI and expressed by GlcNAc challenge

NagI is a member of the LacI family of transcriptional regulators, which generally function as a repressor [24]. Thus, we speculate that NagI has a negative autoregulation effect on the expression of the *nag* operon. To test this, KJΔNagI (a *nagI* deletion mutant of KJ) and the plasmid pNagP$_{xylE}$ (a P_{nagP}-*xylE* transcriptional fusion construct) were prepared. The C23O activity expressed by KJΔNagI(pNagP$_{xylE}$) showed a 8.1 ± 1.1-fold increase compared to that expressed by KJ(pNagP$_{xylE}$) (Fig. 5A),

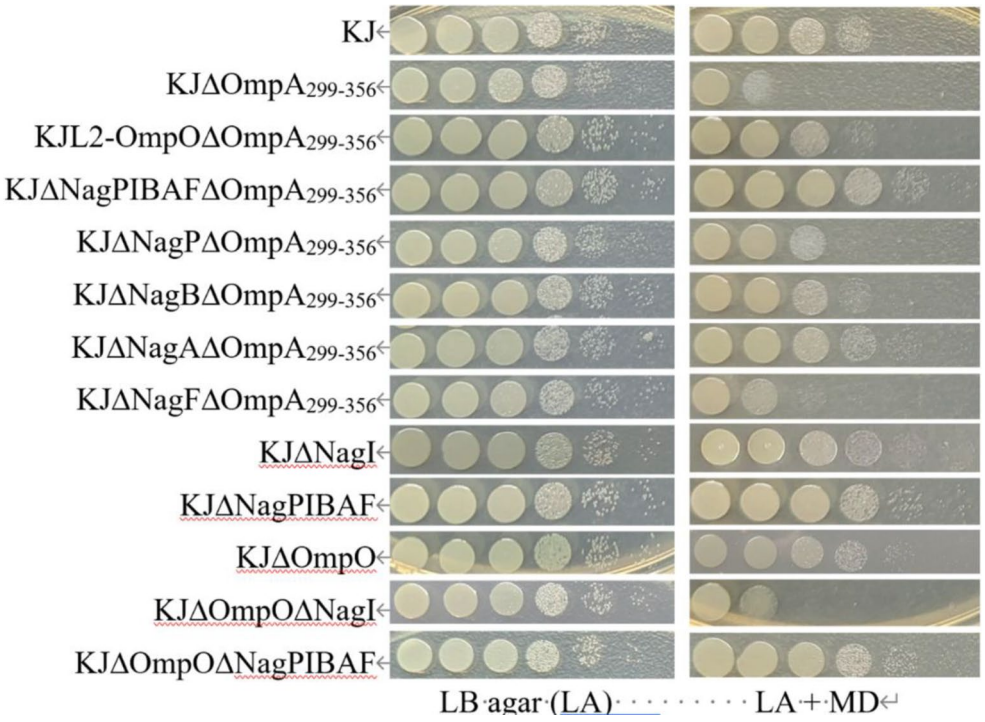

Fig. 4 Menadione tolerance of wild-type KJ and its derived mutants. Bacterial cells (2×10^5 CFU/μL) were 10-fold serially diluted and 5 μL bacterial aliquots were spotted onto LB agar plates with and without 40 μg/mL menadione. After 24-h incubation at 37 °C, bacterial viability was imaged. The graph is a representative of five replicated experiments

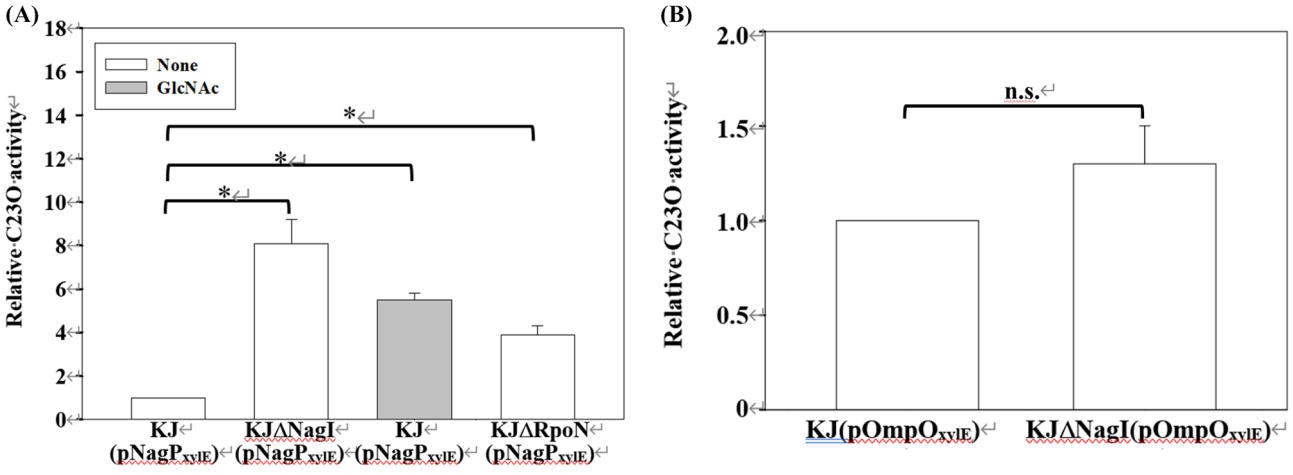

Fig. 5 The regulation of *nagPIBAF* operon. Overnight cultures of the tested bacteria were inoculated into fresh LB at an initial OD_{450nm} of 0.15 and then cultured for 5 h. The enzyme activity of catechol 2,3-dioxygenase encoded by the *xylE* gene was determined using catechol as the substrate. One unit of enzyme activity (U) is defined as the amount of C23O that converts 1 nmole catechol per min. The C23O specific activity is expressed as U/OD_{450nm}. Relative C23O activity was calculated using the C23O level of KJ cells as 1. Data is the means from three independent experiments. Bars represent the average values from three independent experiments. Error bars represent the standard deviation for triplicates. *, $P<0.001$, significance calculated by Student's *t*-test. n.s., nonsignificant. (**A**) The roles of NagI, GlcNAc, and RpoN in the expression of *nagPIBAF* operon. GlcNAc added was 100 mM. (**B**) The role of NagI in *ompO* expression

indicating that NagI functions as a repressor and negatively regulates the expression of *nag* operon.

Given the contribution of *nag* operon to GlcNAc utilization (Supplemental Fig. 2), we were interested in whether *nag* operon can be expressed upon the challenge of GlcNAc. The C23O activities of KJ($pNagP_{xyE}$) with and without the treatment of GlcNAc were determined. In the presence of GlcNAc, the C23O activity of KJ($pNagP_{xylE}$) was significantly increased (Fig. 5A).

In addition, the possibility that there is a separate promoter located upstream of the *nagI* gene was considered. A promoter-*xylE* transcriptional fusion construct pNagI-$_{xylE}$ was prepared. The C23O activities of KJ(pNagI$_{xylE}$) and KJΔNagI(pNagI$_{xylE}$) were determined. No significant C23O activity was observed (Supplemental Fig. 3), tentatively ruling out the presence of individual promoter for *nagI* gene.

NagP, *nagB*, and *naga* upregulation contributes to the Δ*ompA*$_{299-356}$-mediated decrease of MD tolerance

To further elucidate the individual contribution of the *nag* operon members to Δ*ompA*$_{299-356}$-mediated decrease of MD tolerance, Δ*nagP*, Δ*nagB*, Δ*nagA*, and Δ*nagF* were individually introduced into KJΔOmpA$_{299-356}$ and the resultant mutants were subjected to an MD tolerance assay. No polar effect on these mutants was observed, verified by qRT-PCR (Supplemental Fig. 4). KJΔNagPΔOmpA$_{299-356,}$ KJΔNagAΔOmpA$_{299-356,}$ and KJΔNagBΔOmpA$_{299-356}$, but not KJΔNagFΔOmpA$_{299-356,}$ partially restored MD tolerance to the wild-type level (Fig. 4), indicating that NagP, NagA, and NagB upregulation in KJΔOmpA$_{299-356}$ contributes to *DompA*$_{299-356}$-mediated decrease of MD tolerance.

Next, we wondered whether *nag* operon upregulation in wild-type KJ was linked to compromised MD tolerance. Given that NagI functions as a repressor of *nag* operon expression, the MD tolerance of KJΔNagI and KJΔNagPIBAF was assessed. KJΔNagI and KJΔNagPIBAF displayed MD tolerance comparable to wild-type KJ (Fig. 4). Collectively, the contribution of *nag* operon upregulation to MD tolerance decrease is observed in the Δ*ompA*$_{299-356}$ background, but not in the wild-type background.

Nag operon upregulation and *ompO* downregulation synergistically contribute to the Δ*ompA*$_{299-356}$-mediated decrease of MD tolerance

In our previous study, we demonstrated that *ompO* downregulation participates in the Δ*ompA*$_{299-356}$-mediated decrease of MD tolerance. However, deletion of *ompO* in the wild-type background did not influence MD tolerance [18]. In this study, similar observation was noticed that *nag* operon upregulation contributes to MD tolerance decrease in the Δ*ompA*$_{299-356}$ background, but not in the wild-type background (Fig. 4). These observations led us to speculate whether the simultaneous *ompO* downregulation and *nag* operon upregulation result in MD tolerance decrease in wild-type background. To test this possibility, we constructed a *nagI* and *ompO* double-deletion mutant, KJΔOmpOΔNagI, in which the *nag* operon was upregulated and no OmpO protein was translated. Compared with wild-type KJ, KJΔOmpOΔNagI decreased MD tolerance; however, individual inactivation of *nagI* or *ompO* hardly affected MD tolerance in the wild-type background (Fig. 4). To further verify the significance of *nagPIBAF* upregulation in KJΔOmpOΔNagI, KJΔOmpOΔNagPIBAF was constructed. Compared to that of KJΔOmpOΔNagI, the MD tolerance of KJΔNagPIBAFΔOmpO was reverted to the wild-type level (Fig. 4). In summary, *nag* operon upregulation and *ompO* downregulation synergistically contributed to MD tolerance decrease in wild-type KJ.

To further confirm the link between *nag* operon, *ompO*, and MD-mediated oxidative stress, the intracellular ROS levels in KJ and its derived constructs with and without MD challenge were determined. In the absence of MD, all constructs displayed intracellular ROS levels comparable to those of wild-type KJ (Fig. 6A). In the presence of MD, KJΔOmpA$_{299-356}$ had an increased intracellular ROS level. The ROS level of KJΔOmpA$_{299-356}$ was reverted to the wild-type KJ level when *nagPIBAF* operon was deleted or *ompO* was overexpressed in KJΔOmpA$_{299-356}$ (KJΔNagPIBAFΔOmpA$_{299-356}$ and KJL2-OmpOΔOmpA$_{299-356}$ in Fig. 6B). In the wild-type KJ background, the intracellular ROS levels of KJΔOmpOΔNagI increased. However, neither KJDOmpO nor KJΔNagI changed intracellular ROS levels compared to wild-type KJ (Fig. 6B).

σ^N negatively regulates *nag* operon expression

Based on our previous findings that *rpoN* downregulation and *ompO* upregulation contribute to Δ*ompA*$_{299-356}$-mediated decrease of MD tolerance and *ompO* is not a member of σ^N regulon [18] (Fig. 2), we speculated *nag* operon may be a member of σ^N regulon. To test this hypothesis, *nag* operon expression in *rpoN* mutant was assessed. Inactivation of *rpoN* upregulated *nag* operon expression (Fig. 5A), indicating a negative role for σ^N in *nag* operon expression.

It has been verified that *rpoN* downregulation is a critical determinant for swimming compromise in KJΔOmpA$_{299-356}$ [18] (Fig. 2). Furthermore, the above results supported that *nag* operon is a member of σ^N regulon. Therefore, the involvement of *nag* operon in swimming motility was investigated. Compared with wild-type KJ, KJΔOmpA$_{299-356}$ displayed decreased swimming motility, and this compromise was not significantly changed in KJΔNagPIBAFΔOmpA$_{299-356}$ (Supplemental Fig. 5), indicating *nag* operon upregulation in KJΔOmpA$_{299-356}$ is irrelated to swimming compromise.

NagI does not influence the expression of *ompO*

Given the involvement of *nag* operon and *ompO* in MD tolerance (Fig. 4), we investigated whether NagI had an impact on *ompO* expression. The *ompO* expression in KJ and KJΔNagI cells was comparable (Fig. 5B),

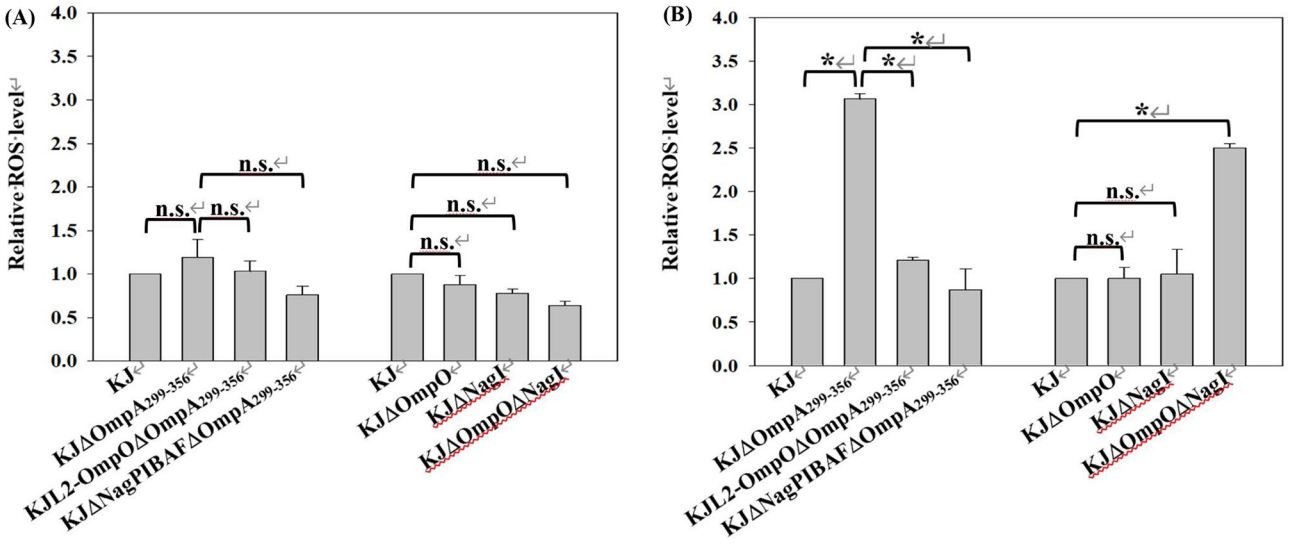

Fig. 6 The ROS levels of wild-type KJ and its derived constructs. Bacterial cells tested were cultured in LB medium with and without MD of 16 μg/mL for 4 h. DCFH-DA was added to a final concentration 0.01 μM. After 1-h culture, the fluorescence intensity at 520 nm was determined. The relative fluorescence is normalized to the fluorescence of wild-type KJ. *, $P < 0.01$, significance calculated by Student's *t*-test. n.s., nonsignificant. (**A**) ROS levels of wild-type KJ and its derived constructs grown in LB. (**B**) ROS levels of wild-type KJ and its derived constructs grown in LB with 16 μg/mL MD

tentatively ruling out the regulatory role of NagI in *ompO* expression.

Discussion

The PG recycling and GlcNAc metabolism are intimately linked in gram-negative bacteria. GlcN-6P is a critical intermediate that can be driven to PG recycling via the GlmM-GlmU pathway or to glycolysis by NagB (Fig. 1). Thus, upregulation of the *nagPIBAF* operon in KJΔOmpA$_{299-356}$ can favor GlcN-6P shift to the route of glycolysis, which may lead to an increase in ROS levels (Fig. 1). From the transcriptome results, we also noticed that a lot of carbohydrate metabolism-associated genes are also upregulated in KJΔOmpA$_{299-356}$, in addition to *nagPIBAF* operon, for example hexose kinase (encoded by *smlt2557*), carbohydrate kinase (encoded by *smlt2183*), and glycoside hydrolases (encoded by smlt2180 and 2185). Thus, the increase of endogenous ROS level in KJΔOmpA$_{299-356}$ may result from not only *nagP-nagA-nagB* circuit but also other carbohydrate metabolism in KJΔOmpA$_{299-356}$. In addition, in response to ROS stress, a variety of alleviation systems are triggered, including ROS degradation and exportation [3]. Based on the transcriptome results, *ompO* downregulation can be the dominant factor contributing to Δ*ompA*$_{299-356}$-mediated MD tolerance decrease since the expression of other known oxygen stress alleviation systems are not significantly altered [18]. OmpO is a β-barrel outer membrane protein, which generally functions as a channel for the influx or efflux of molecules [25]. Thus, we assumed that OmpO is an outlet for ROS or toxic compounds generated by ROS. Therefore, *nagPIBAF* upregulation can increase glycolytic activity, and *ompO* downregulation may decrease the export of oxidative stress-mediated toxic molecules, both synergistically resulting in MD tolerance decrease. The finding of *ompO* downregulation and *nagPIBAF* upregulation in KJΔOmpA$_{299-356}$ was disclosed via transcriptome analysis; thus, we cannot immediately rule out the possibility that there are some unidentified regulatory circuits, which may be involved in the translation level, responsible for Δ*ompA*$_{299-356}$-mediated MD tolerance decrease.

LacI family transcription regulators generally function as global regulators of sugar metabolism. Furthermore, *lacI* and the sugar metabolism-associated genes are generally clustered. The majority of LacI family members are repressors. When they perceive sugar effectors and, in response, derepress the expression of the genes involved in the use of carbohydrates. In this study, we elucidated that *nagPIBAF* operon, but not *ompO*, is the member of *nagI* regulon, which is well consistent with the perception of LacI regulator. Based on the known functions of NagP of *X. campestris* [10] and NagA-NagB system of *E. coli* [26], we presumed that GlcNAc and (or) GlcNAc-derived metabolites are highly the sugar effectors to derepress *nag* operon in *S. maltophilia*. The involvement of *nag* operon in GlcNAc utilization (Supplemental Fig. 2) and the derepression of *nag* operon by GlcNAc (Fig. 5A) further strengthen this aspect. The C-terminal domain of OmpA is associated with PG layer, contributing to the maintenance of PG stability [11]. GlcNAc is the sugar component of PG monomer [6]. Thus, loss of the OmpA-PG interaction may cause the disturbance of PG homeostasis and increase the GlcNAc level in periplasm, leading

to the depression of *nag* operon. This rationale may also provide an explanation why only *nagP*, *nagA*, and *nagB*, but not *nagF* involve in $\Delta ompA_{299-356}$-mediated decrease of MD tolerance (Fig. 4) since *nagF* may less relate to GlcNAc utilization in our assay systems.

NagA and NagB are well-known enzymes participating in GlcNAc metabolism in bacteria [10, 26, 27]. In addition, the significance of NagA and NagB in other functions is also reported. For example, the involvement of NagA and NagB of *Staphylococcus aureus* in oxacillin and methicillin susceptibility [28], and NagB of *Streptococcus mutans* in virulence [29]. In this study, we firstly revealed the linkage between NagA and NagB of *S. maltophilia* and oxidative stress tolerance in an $\Delta ompA_{299-356}$ mutant (Fig. 4).

Based on the MD tolerance assay (Fig. 4) and intracellular ROS level determination (Fig. 6), we noticed that the impact of *nagPIBAF* upregulation and *ompO* downregulation on MD tolerance and ROS levels was only observed in MD-treated KJ cells, not in MD-untreated counterpart (Figs. 4 and 6B). This indicates that the oxidative stress alleviation systems of *S. maltophilia* are sufficient to deal with *nagPIBAF* upregulation- and *ompO* downregulation-generated oxidative stress if no external oxidative stress is imposed. However, when external oxidative stress, *nagPIBAF* upregulation, and *ompO* downregulation coexist, such as MD-treated $KJ\Delta OmpA_{299-356}$ cells, the accumulated oxidative stress exceeds the capacity of oxidative stress alleviation systems and affects bacterial growth.

Conclusion

$KJ\Delta OmpA_{299-356}$, an *ompA* deletion mutant of *S. maltophilia* KJ, exhibits compromised MD tolerance, and σ^E, σ^N, and OmpO are involved in this regulatory circuit [18] (Fig. 2). Integrating previous findings with the results of this study, we expanded the understandings on the regulatory mechanism responsible for $\Delta ompA_{299-356}$-mediated decrease of MD tolerance (Fig. 2). OmpA is the most abundant outer-membrane protein in *S. maltophilia* KJ. The 299–356 amino acid residues of OmpA are key domains for the interaction between OmpA and PG. Thus, OmpA of $KJ\Delta OmpA_{299-356}$ loses contact with the PG, which causes envelope stress and triggers σ^E activation. Sigma E activation downregulates *ompO* and *rpoN* expression. Furthermore, *rpoN* downregulation upregulates *nagPIBAF* operon. *OmpO* downregulation and *nagPIBAF* upexpression contribute to $\Delta ompA_{299-356}$-mediated decrease of MD tolerance; nevertheless, there is no cross-regulation between NagI and *ompO* (Fig. 2).

Supplementary Information

The online version contains supplementary material available at https://doi.org/10.1186/s12866-025-03840-9.

Supplementary Material 1

Acknowledgements
Not applicable.

Author contributions
TC Yang and LH Li wrote the main manuscript text. HF Lu and YT Lin prepared Table 1; Figs. 1 and 2. TC Yang, SC Wu, and TY Yeh prepared Figs. 3, 4, 5 and 6 and supplemental materials. All authros reviewed the manuscript.

Funding
This project has received funding from the National Science and Technology Council of Taiwan (grant numbers NSTC 112-2320-B-075-005 and NSTC 113-2320-B-075-008) and the Taipei Veterans General Hospital (grant number V113C-225).

Data availability
All data generated or analyzed during this study are included in this published article and its supplementary information files.

Declarations

Ethics approval and consent to participate
Not applicable.

Consent for publication
Not applicable.

Competing interests
The authors declare no competing interests.

Author details
[1]Department of Biotechnology and Laboratory Science in Medicine, National Yang Ming Chiao Tung University, Taipei, Taiwan, Republic of China
[2]Department of Medical Laboratory Science and Biotechnology, Asia University, Taichung, Taiwan, Republic of China
[3]Division of Infectious Diseases, Department of Medicine, Taipei Veterans General Hospital, Taipei, Taiwan, Republic of China
[4]School of Medicine, National Yang Chiao Tung University, Taipei, Taiwan, Republic of China
[5]Department of Pathology and Laboratory Medicine, Taipei Veterans General Hospital, Taipei, Taiwan, Republic of China
[6]School of Medical Laboratory Science and Biotechnology, College of Medical Science and Technology, Taipei Medical University, Taipei, Taiwan, Republic of China

Received: 30 September 2024 / Accepted: 21 February 2025
Published online: 07 March 2025

References

1. Imlay JA. The molecular mechanisms and physiological consequences of oxidative stress: lessons from a model bacterium. Nat Rev Microbiol. 2013;11:443–54.
2. Chevallier V, Andersen MR, Malphettes L. Oxidative stress-alleviating strategies to improve Recombinant protein production in CHO cells. Biotechnol Bioeng. 2020;117:1172–86.
3. Lushchak VI. Oxidative stress and mechanisms of protection against it in bacteria. Biochem (Mosc). 2001;66:476–89.
4. Gaupp R, Ledala N, Somerville GA. Staphylococcal response to oxidative stress. Front Cell Infect Microbiol. 2012;2:33.

5. Moye ZD, Burne RA, Zeng L. Uptake and metabolism of *N*-acetylglucosamine and glucosamine by *Streptococcus* mutans. Appl Environ Microbiol. 2014;80:5053–67.
6. Park JT, Uehara T. How bacteria consume their own exoskeletons (turnover and recycling of cell wall peptidoglycan). Microbiol Mol Biol Rev. 2008;72:211–7.
7. Cheng Q, Li H, Merdek K, Park JT. Molecular characterization of the beta-*N*-acetylglucosaminidase of *Escherichia coli* and its role in cell wall recycling. J Bacteriol. 2000;182:4836–40.
8. Rogers MJ, Ohgi T, Plumbridge J, Soll D. Nucleotide sequences of the *Escherichia coli NagE* and *NagB* genes: the structural genes for the *N*-acetylglucosamine transport protein of the bacterial phosphoenolpyruvate: sugar phosphotransferase system and for the glucosamine-6-phosphate deaminase. Gene. 1988;62:197–207.
9. Xiao X, Wang F, Saito A, Majka J, Schlosser A, Schrempf H. The novel *Streptomyces olivaceoviridis* ABC transporter Ngc mediates uptake of *N*-acetylglucosamine and *N*, *N*′-diacetylchitobiose. Mol Genet Genomics. 2002;267:429–39.
10. Boulanger A, Déjean G, Lautier M, Glories M, Zischek C, Arlat M, Lauber E. Identification and regulation of the *N*-acetylglucosamine utilization pathway of the plant pathogenic bacterium *Xanthomonas campestris* Pv. campestris. J Bacteriol. 2010;192:1487–97.
11. Pautsch A, Schulz GE. Structure of the outer membrane protein A transmembrane domain. Nat Struct Biol. 1998;5:1013–7.
12. Mot R, Vanderleyden J. The C-terminal sequence conservation between OmpA-related outer membrane proteins and MotB suggests a common function in both Gram-positive and Gram-negative bacteria, possibly in the interaction of these domains with peptidoglycan. Mol Microbiol. 1994;12:333–4.
13. Confer AW, Ayalew S. The OmpA family of proteins: roles in bacterial pathogenesis and immunity. Vet Microbiol. 2013;163:207–22.
14. Guan Q, Bhowmick B, Upadhyay A, Han Q. Structure and functions of bacterial outer membrane protein A, a potential therapeutic target for bacterial infection. Curr Top Med Chem. 2021;21:1129–38.
15. Dekoninck K, Létoquart J, Laguri C, Demange P, Bevernaegie R, Simorre JP, Dehu O, Iorga BI, Elias B, Cho SH, Collet JF. Defining the function of OmpA in the Rcs stress response. Elife. 2020;9:e60861.
16. Liao CH, Chang CL, Huang HH, Lin YT, Li LH, Yang TC. Interplay between OmpA and RpoN regulates flagellar synthesis in *Stenotrophomonas maltophilia*. Microorganisms. 2021;9:1216.
17. Li LH, Wu CM, Chang CL, Huang HH, Wu CJ, Yang TC. σ^P-NagA-L1/L2 regulatory circuit involved in $\Delta ompA_{299\text{-}356}$-mediated Increase in β-lactam susceptibility in *Stenotrophomonas maltophilia*. Microbiol Spectr. 2022;10:e02797–22.
18. Ku RH, Li LH, Liu TF, Hu EW, Lin YT, Lu HF, Yang TC. Implication of the σ^E regulon members OmpO and σ^N in the $\Delta ompA_{299–356}$-mediated decrease of oxidative stress tolerance in *Stenotrophomonas maltophilia*. Microbiol Spectr. 2023;11:e01080–23.
19. Yang TC, Huang YW, Hu RM, Huang SC, Lin YT. AmpDI is involved in expression of the chromosomal L1 and L2 b-lactamases of *Stenotrophomonas maltophilia*. Antimicrob Agents Chemother. 2009;53:2902–7.
20. Chen CH, Huang CC, Chung TC, Hu RM, Huang YW, Yang TC. Contribution of resistance-nodulation-division efflux pump Operon *smeU1-V-W-U2-X* to multidrug resistance of *Stenotrophomonas maltophilia*. Antimicrob Agents Chemother. 2011;55:5826–33.
21. Hu RM, Huang KJ, Wu LT, Hsiao YJ, Yang TC. Induction of L1 and L2 b-lactamases of *Stenotrophomonas maltophilia*. Antimicrob Agents Chemother. 2008;52:1198–200.
22. Rajneesh PJ, Chatterjee A, Singh SP, Sinha RP. Detection of reactive oxygen species (ROS) in Cyanobacteria using the oxidant-sensing probe 2′,7′-dichlorodihydrofluorescein diacetate (DCFH-DA). Bio Protoc. 2017;7:e2545.
23. Messner KR, Imlay JA. The identification of primary sites of superoxide and hydrogen peroxide formation in the aerobic respiratory chain and sulfite reductase complex of *Escherichia coli*. J Biol Chem. 1999;274:10119–28.
24. Ravcheev DA, Khoroshkin MS, Laikova ON, Tsoy OV, Sernova NV, Petrova SA, Rakhmaninova AB, Novichkov PS, Gelfand MS, Rodionov DA. Comparative genomics and evolution of Regulons of the LacI-family transcription factors. Front Microbiol. 2014;5:294.
25. Koebnik R, Locher KP, van Gelder P. Structure and function of bacterial outer membrane proteins: barrels in a nutshell. Mol Microbiol. 2000;37:239–53.
26. Alvarez-Anorve LI, Bustos-Jaimes I, Calcagno ML, Plumbridge J. Allosteric regulation of glucosamine-6-phosphate deaminase (NagB) and growth of *Escherichia coli* on glucosamine. J Bacteriol. 2009;191:6401–7.
27. Afzal M, Shafeeq S, Manzoor I, Henriques-Normark B, Kuipers OP. *N*-acetylglucosamine-mediated expression of *NagA* and *NagB* in *Streptococcus pneumoniae*. Front Cell Infect Microbiol. 2016;6:158.
28. Komatsuzawa H, Fujiwara T, Nishi H, Yamada S, Ohara M, McCallum N, Berger-Bachi B, Sugai M. The gate controlling cell wall synthesis in *Staphylococcus aureus*. Mol Microbiol. 2004;53:1221–31.
29. Kawada-Matsuo M, Mazda Y, Oogai Y, Kajiya M, Kawai T, Yamada S, Miyawaki S, Oho T, Komatsuzawa H. GlmS and NagB regulate amino sugar metabolism in opposing directions and affect Streptococcus mutans virulence. PLoS ONE. 2012;7:e33382.

Publisher's note